

Computer Simulations of the ESR Spectra of the Triplet Dimers of Bis-(*N*-Salicylidene-methylaminato)copper(II) in Toluene

Makoto CHIKIRA and Taro ISOBE

Chemical Research Institute of Non-aqueous Solutions, Tohoku University, Katahira, Sendai

(Received January 31, 1972)

It has been concluded, from computer simulations of the observed ESR line shapes, that the dimeric structure of bis-(*N*-salicylidene-methylaminato)copper(II) in a frozen toluene solution is similar to that in its γ -form crystals. Furthermore, the difference between the hyperfine splittings observed at both edges of the triplet spectra for $\Delta M = 1$, the large frequency dependence of the fine-structure splitting, and the additional hyperfine structures observed in the field range between the so-called low-field parallel and perpendicular lines have been found to be due to the noncoincidence of the principal axes of the g tensor with those of the fine-structure tensor.

The ESR spectra of the triplet dimers of copper complexes in frozen solutions have been studied by many authors.¹⁻⁷⁾ Although there are a variety of dimeric structures, it has always been assumed that the spin Hamiltonian applied to the dimers is axially symmetric and that the principal axes of the g tensor are coincident with those of the fine-structure tensor, D . Recently, Yokoi and Isobe⁷⁾ found that triplet dimers are formed at considerably high concentrations in the toluene solutions of some 1 : 2 β -diketone chelate complexes of copper(II) and that the dimers are in equilibrium with the monomers. We established that such an equilibrium exists in the toluene solution of bis-(*N*-salicylidene-methylaminato)copper(II) (abbreviated as Cu(Mesal)₂). Furthermore, its ESR line shapes at 77°K could not be explained in terms of the spin Hamiltonian usually applied.

The dimeric structure shown in Fig. 1 is found in the γ -form crystals of Cu(Mesal)₂.⁸⁾ It can naturally be supposed that the complex in toluene has the same di-

meric structure as in the γ -form crystals. The axes of the fine-structure tensor due to magnetic dipole interactions in such a dimer do not coincide with those of the g tensor. The purpose of this paper, therefore, is to estimate the dimeric structure of the complex in toluene on the basis of computer simulations of the ESR line shapes of randomly-oriented triplet dimers, using a more general spin Hamiltonian.

Experimental

The ESR spectra of Cu(Mesal)₂ in toluene were recorded at 77°K with two HITACHI ESR spectrometers, Model 771 (X-band) and Model MES 4001 (K-band). The field was calibrated with an NMR probe and then with a benzene solution of vanadyl acetylacetonate. Cu(Mesal)₂ was prepared according to the method in the literature⁹⁾ and was recrystallized from methanol several times.

Results and Discussion

ESR Spectra of the Triplet Dimers. The X-band and K-band ESR spectra of Cu(Mesal)₂ in toluene measured at 77°K are shown in Figs. 2, 3, and 4. The spectra in Figs. 2 and 4 consist of two kinds of spectra; one is due to monomer species ($S=1/2$), and the other, to triplet dimer species ($S=1$). Various magnetic parameters are defined in these figures; A_3 is the hyperfine splitting constant of the so-called⁴⁾ minimum-field lines of $\Delta M=2$ transitions, A_L and A_H are those of the low-field and high-field parallel lines of $\Delta M=1$

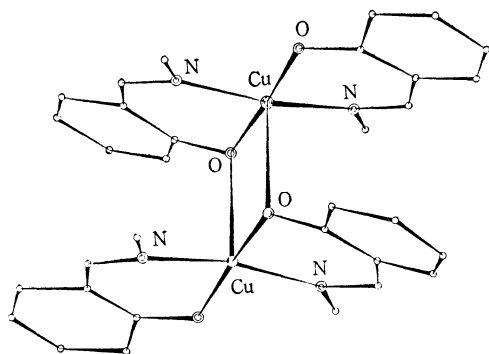


Fig. 1. Structure of the dimer in the γ -form crystals⁸⁾ of Cu(Mesal)₂.

1) R. H. Dunhill, J. R. Pilbrow, and T. D. Smith, *J. Chem. Phys.*, **45**, 1474 (1961).

2) J. F. Boas, R. H. Dunhill, and J. R. Pilbrow, *J. Chem. Soc., A*, **1969**, 94.; J. F. Boas, J. H. Price, J. R. Pilbrow, K. S. Murray, and T. D. Smith, *ibid.*, **A**, **1970**, 968.

3) G. F. Kokoszka, M. Linzer, and G. Gordon, *Inorg. Chem.*, **7**, 1730 (1968).

4) N. D. Chasteen and R. L. Belford, *ibid.*, **9**, 169 (1970).

5) W. E. Hatfield, J. A. Barnes, D. Y. Jeter, R. Whymann, and E. R. Jones, Jr., *J. Amer. Chem. Soc.*, **92**, 4982 (1970).

6) G. O. Carlisle and W. E. Hatfield, *Inorg. Nucl. Chem. Lett.*, **6**, 633 (1970); J. F. Villa and W. E. Hatfield, *Inorg. Chim. Acta*, **5**, 145 (1971).

7) H. Yokoi and T. Isobe, *This Bulletin*, **44**, 1446 (1971); *ibid.*, to be published.

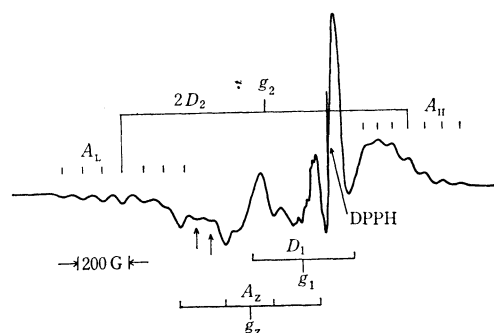


Fig. 2. The X-band ESR spectrum of Cu(Mesal)₂ in toluene at 77°K (0.01 M).

8) D. Hall, S. V. Sheat, and T. N. Water, *J. Chem. Soc., A*, **1968**, 460.

9) P. Peifer and H. Glaser, *J. Prakt. Chem.*, **153**, 265 (1939).

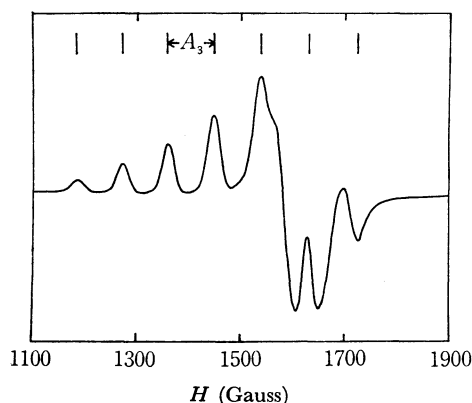


Fig. 3. "Half-field" $\Delta M=2$, ESR spectrum of $\text{Cu}(\text{Mesal})_2$ in toluene at 77°K (0.1 M).

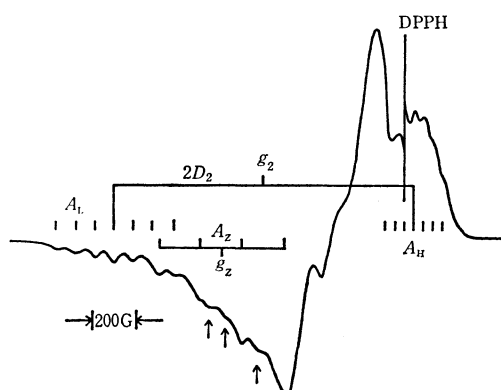


Fig. 4. The K-band ESR spectrum of $\text{Cu}(\text{Mesal})_2$ in toluene at 77°K (0.05 M).

transitions, respectively. D_2 is one half of the splitting between the full-field parallel lines, and D_1 is a splitting between the full-field perpendicular lines. The values of g_1 and g_2 were determined from the centers of the full-field perpendicular and parallel lines respectively. These results are listed in Table 1.

The ESR spectra of the triplet dimers of copper complexes show seven-line hyperfine patterns upon the coupled nuclear spin ($I=3$) of two copper ions ($I=3/2$), and the separations of the hyperfine components can be expected to be about one half of those observed for the monomer.¹⁰ It should be noted that the A_3 , A_L , and A_H at the X-band spectra are all different, and that they decrease in this order. In the K-band spectrum, A_L becomes a little larger, but the A_H is considerably smaller than that in the X-band spectrum. It is also evident that the D_2 in the X-band differs both from the D_1 in the same band and from the D_2 in the K-band. In addition, the g_2 is considerably smaller than the g_z of the monomers. If the dimers were axially symmetric and if the axes of the g , D , and hyperfine tensors were all coincident with each other, A_L and D_2 would have to be almost equal to A_H and D_1 respectively.^{3,4} In this case, therefore, the small difference between A_L and A_H must be attributed to the second-order effect of hyperfine interactions. However, this difference cannot be explained only by this effect, because the second-order effect weakens as the resonance frequency

increases. This fact contradicts the experimental result that the difference between A_L and A_H in the K-band becomes quite a bit larger than that in the X-band. Moreover, we must point out that additional hyperfine structures, which are indicated by arrows in Figs. 2 and 4, were found in the field range between the so-called low-field parallel and perpendicular lines; it is clear that the hyperfine structures are due not to the monomers, but to the dimers. Similar hyperfine structures had been found more clearly in the spectra of the aqueous solutions of copper tartrates at 77°K .⁴ However, these structures have not yet been explained theoretically.

TABLE 1. MAGNETIC PARAMETERS

	Observed values		Case A		Case B	
	X-band	K-band	X-band	K-band	X-band	K-band
A_3	87 G					
A_L	79	82 G	75 G	81 G	80 G	85 G
A_H	65	46	60	51	64	52
g_1	2.069				2.116	2.094
g_2	2.170	2.169	2.126	2.127	2.164	2.186
D_1	394 G				475 G	430 G
D_2	563	657 G	753 G	830 G	560	679

Magnetic parameters of the monomer; $g_z=2.220$, $A_z=0.0192\text{ cm}^{-1}$, $g_0=2.112$, $A_0=0.0079\text{ cm}^{-1}$, where g_0 and A_0 were determined from the X-band spectra at room temperature. (X-band: 9.2202 GHz, K-band: 23.816 GHz).

The resonance conditions of triplet dimers for the $\Delta M=1$ transitions can be expressed by this first-order approximation:¹¹

$$\hbar\omega = g(z, \varphi)\beta H \pm D(z, \varphi) + A(z, \varphi)M_I; z = \cos \theta \quad (1)$$

where θ and φ are the polar co-ordinates of the direction of the static magnetic field, where M_I is the quantum number of the hyperfine component of the coupled nuclear spin, and where ω is the angular frequency of the oscillating magnetic field. Then, the resonance magnetic field can be calculated from Eq. (1) as:

$$H(z, \varphi) = \frac{\hbar\omega \mp D(z, \varphi) - A(z, \varphi)M_I}{g(z, \varphi)\beta} \quad (2)$$

It was indicated by Kottis and Lefebvre¹² that the ESR spectrum of a paramagnetic powder or a glassy solution show characteristic peaks in the fields where the stationary conditions (3) are satisfied:

$$dH = \frac{\partial H}{\partial z} dz + \frac{\partial H}{\partial \varphi} d\varphi = 0 \quad (3)$$

From Eqs. (2) and (3), two stationary conditions for the $\Delta M=1$ transitions can be obtained according to the plus and minus signs in Eq. (2). If the principal axes of the g , D and A tensors are coincident with each other, the two conditions will be simultaneously satisfied in the directions of the tensor axes, because both $\partial H/\partial z$ and $\partial H/\partial \varphi$ always vanish in those directions. If these axes do not coincide with each other, the ori-

11) B. Bleaney, *Phil. Mag.*, **42**, 441, (1951).

12) P. Kottis and R. Lefebvre, *J. Chem. Phys.*, **39**, 393 (1963); *ibid.*, **41**, 379 (1964).

10) C. P. Slichter, *Phil. Mag.*, **42**, 441, (1951).

entations which satisfy Eq. (3) will differ according to the plus or minus sign in Eq. (2), and they will not generally agree with the orientation of the principal axes. In that case, the observed parameters are not the principal values of these tensors. These facts suggest that the unusual behavior of the observed hyperfine and fine-structure splittings is due to the noncoincidence of the principal axes of the g tensor with those of the D tensor. In order to confirm this speculation more quantitatively, computer simulations of the ESR line shapes of the randomly-oriented triplet dimers were performed in this investigation. All the calculations were carried out at the Computer Center of Tohoku University.

Simulations of the ESR Line Shapes. The appropriate spin Hamiltonian for the triplet dimers can be expressed as:

$$\mathcal{H} = \mathbf{H} \cdot \mathbf{g} \cdot \mathbf{S} + \mathbf{H}_d + \mathbf{S} \cdot \mathbf{A} \cdot \mathbf{I} + J \mathbf{S}_1 \cdot \mathbf{S}_2 \quad (4)$$

where $\mathbf{S} = \mathbf{S}_1 + \mathbf{S}_2$, $\mathbf{I} = \mathbf{I}_1 + \mathbf{I}_2$

and:

$$\mathbf{H}_d = \left(\frac{\beta^2}{r^3} \right) \left\{ (\mathbf{g} \mathbf{S}_1 \cdot \mathbf{g} \mathbf{S}_2) - \frac{3}{r^2} (\mathbf{g} \mathbf{S}_1 \cdot \mathbf{r}) (\mathbf{g} \mathbf{S}_2 \cdot \mathbf{r}) \right\} \quad (4a)$$

where \mathbf{S}_1 , \mathbf{S}_2 , \mathbf{I}_1 , and \mathbf{I}_2 are the electron and nuclear spin operators of the copper ions, \mathbf{H}_d is the operator of the spin dipole interaction, \mathbf{r} is the distance between the two ions, and the other symbols have their usual meanings. We assumed here that (a) the g tensors of the two molecules are identical, (b) the spin-exchange interaction parameter, J , is large enough for the coupled electronic and nuclear spin quantum numbers ($S=1$, $I=3$) to be good ones, although the contribution of J to the fine-structure splitting is negligibly small as compared with that of \mathbf{H}_d , (c) the principal axes of the g and the A tensors are coincident with each other, and (d) \mathbf{H}_d can be estimated from a point-dipole approximation.

Our method of calculating the line shapes is essentially the same as that used by many other authors.¹²⁻¹⁶) We first calculated the resonance magnetic fields as a function of the orientation with respect to the static magnetic field, integrated it into the powder pattern, and convoluted it with the derivatives of Gaussian or Lorentzian line shapes. We chose the spin eigenfunctions of the Zeeman and exchange interaction terms for a basis set, and regarded \mathbf{H}_d and \mathbf{SAI} as small perturbations. The line shapes of the $\Delta M=2$ transitions in the X-band will not be discussed here. In the case of the $\Delta M=2$ transitions, the amount of Zeeman splitting is not large enough, as compared with the fine-structure or hyperfine splittings, for the perturbation calculations to give proper energy levels. Since the angular dependence of the transition probability cannot be neglected, it is necessary to solve the higher-order secular equations in order to obtain the exact energy levels and matrix elements of the transition moments.

13) E. Wasserman, L. C. Snyder, and W. A. Yager, *J. Chem. Phys.*, **41**, 1736 (1964).

14) F. K. Kneubuhl, *ibid.*, **35**, 156 (1961).

15) R. Neiman and D. Kivelson, *ibid.*, **35**, 156 (1961).

16) P. C. Taylor and P. J. Bary, *J. Mag. Res.*, **2**, 305 (1970); Line Shape Program Manual, 1968, unpublished.

The perturbation calculations were made to the second order for \mathbf{H}_d and to the first order for \mathbf{SAI} . As Fig. 5 shows, the x , y , and z axes of the Cartesian co-ordinates were chosen as the principal axes of the g and A tensors. The directions of the static magnetic field and of the copper-copper axes are expressed by the polar co-ordinates, (θ, φ) and (ξ, η) respectively.

Figure 6 shows the angular dependence of the resonance magnetic field for the $\Delta M=1$ transitions for the $M_I=0$ hyperfine component. The parameters used in these calculations were estimated from the parameters of the monomer species and from the structure of the γ -form crystals. These adopted parameters

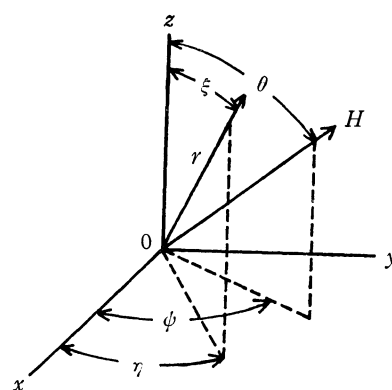


Fig. 5. The directions of the external magnetic field and copper axis with respect to the principal axes of g and A tensors.

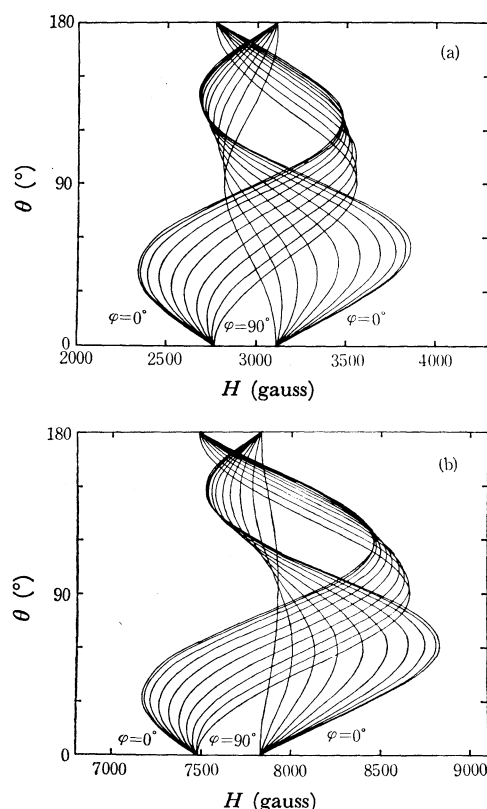


Fig. 6. The angular dependence of the resonance magnetic field of the $\Delta M=1$ transitions for the $M_I=0$ hyperfine component. (a) For X-band, (b) for K-band; $g_{\perp}=2.04$, $\xi=45^{\circ}48'$, $\eta=0^{\circ}$, $r=3.4 \text{ \AA}$.

may not be accurate. It is considered, however, that they do not differ from the exact ones greatly enough for the essential features of the line shapes to disappear, because the electronic states of this complex are not changed very much by the weak dimerization force. As is clearly shown in these figures, the dimers which are resonating at both edges of the $\Delta M=1$ spectra are differently oriented; their θ values are different. The approximate values of A_L , A_H , D_2 , and g_2 , which are defined in Figs. 2 and 4, can be estimated from these figures. If we put $A_{//}=0.0095 \text{ cm}^{-1}$ and $A_{\perp}=0.0010 \text{ cm}^{-1}$, values which are about one half of those observed for the monomers, A_L and A_H can be calculated from Eq. (5),¹¹ as is shown in Case A of Table 1:

$$gA = \sqrt{A_{//}^2 g_{//}^2 \cos^2 \theta + A_{\perp}^2 g_{\perp}^2 \sin^2 \theta} \quad (5)$$

These values agree satisfactorily with the observed values. D_2 and g_2 values similarly obtained from the figures are also tabulated there. These values do not agree with the experimentally-obtained values quantitatively, as the A values do, but they do agree qualitatively. For instance, in both the calculations and the experiment, the D_2 in the X-band is smaller than that in the K-band, and the g_2 is significantly smaller than the g_z usually observed for various five-co-ordinated copper complexes. These facts suggest that the structures of the dimers in toluene are very similar to those in the γ -form crystals. In order to determine the parameters more precisely, A_L , A_H , g_2 , and D_2 were estimated graphically at different values of r and ξ . First of all, we will discuss the behaviors of g_2 and D_2 . From Eq. (1), g_2 and D_2 can be expressed to the first-order approximation:

$$g_2 = \frac{2g_L g_H}{g_L + g_H} \quad (6)$$

and:

$$2D_2 = \frac{\hbar\omega}{\beta} \left(\frac{1}{g_H} - \frac{1}{g_L} \right) + \frac{1}{\beta} \left(\frac{D_H}{g_H} - \frac{D_L}{g_L} \right) \quad (7)$$

where g_L , g_H , D_L , and D_H are the g factors and the fine-structure splittings of the dimers, whose orientations can be determined graphically from the minimum and maximum resonance fields of the $\Delta M=1$ transitions. Practically, g_2 is almost equal to $g(\xi, \eta)$. The difference between g_L and g_H becomes larger as the anisotropy of the g tensor, the frequency of the oscillating magnetic field, and the gaps between the copper-copper axis and g tensor axes increase. Accordingly, the first term of Eq. (7) varies greatly with the microwave frequency. On the other hand, the values of the second term changes only a little with the frequency. If the fine-splittings are due only to the magnetic dipole interactions, the value of the second term will be approximately determined by the distance between the two cupric ions and, therefore, somewhat affected by a change in the ξ value. In the X-band spectra, the first term of Eq. (7) is negligibly small as compared with the second one. In this case, the D_2 in the X-band almost agrees with one of the principal values of the zero-field splitting tensor, which is usually represented as Eq. (8) for a point-dipole interaction:

$$D_{d-a} = \frac{3}{4} g^2 \beta^2 \left\{ \frac{1 - 3 \cos^2 \theta}{r^3} \right\}_{\max} \quad (8)$$

Accordingly, the distance between the two cupric ions in the dimers can be calculated from Eq. (8) to be 3.39 Å, using the value of g_2 and D_2 obtained from Fig. 6. It is almost the same as the value of r (3.4 Å) used for the calculations in Fig. 6. The ξ and r dependence of D_2 is shown in Fig. 7. As is evident from Fig. 7, the ξ dependence of D_2 in the K-band is larger than that in the X-band. When ξ is closer to 0° or 90° , the difference between the D_2 values in the X-band and the K-band becomes very small. In other words, if the difference is large and the second-order effect of the fine-structure tensor is negligible, there will be a large gap between the copper-copper and g tensor axes.

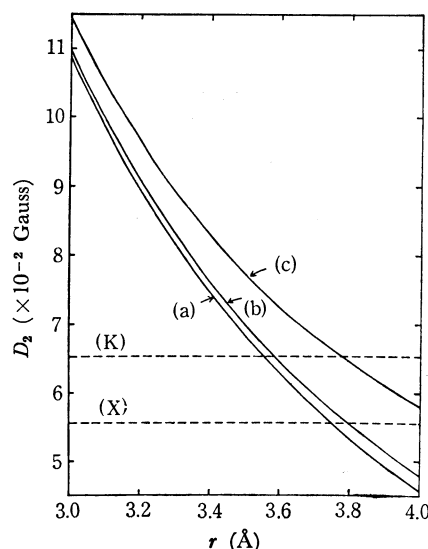


Fig. 7. The relation between D_2 and r . $g_{//}=2.22$, $g_{\perp}=2.04$; As ξ changes $0^\circ \rightarrow 90^\circ$, D_2 changes (a) \rightarrow (b) \rightarrow (a) at X-band, and (a) \rightarrow (c) \rightarrow (a) at K-band. The broken lines, (K) and (X), indicate the observed values of D_2 at K-band and X-band, respectively.

Next, we will discuss the hyperfine structures of the so-called full-field parallel lines. The dependence of A_L and A_H on r for different values of ξ in the X-band is shown in Fig. 8. This figure indicates that the calculated values of A_L and A_H depend sharply on ξ , but that they do not change greatly with r at any of the ξ values. In these figures, the observed values of A_L and A_H are also indicated. The approximate values of ξ could be estimated from these figures to be between 30° and 40° . The difference between A_L and A_H increases with the increase in the anisotropy of the g tensor. The relations between ΔA and Δg can be understood well from Fig. 9, where $\Delta A = A_L - A_H$ is plotted against ξ for different values of $\Delta g = g_L - g_H$. As is evident from these figures, the change in ΔA with Δg depends on the ξ angle and on the frequency of the oscillating magnetic field. It also depends naturally on the anisotropy of the A tensor. When the shift of the spectral lines due to the anisotropy of the g tensor is smaller than that due to the fine-structure tensor, ΔA becomes zero at $\xi=0^\circ$ and 90° . This condition is not satisfied in the case of (5) in the K-band in Fig. (9). In this case, the $(-1 \rightarrow 0)$ transition at the minimum resonance field or the $(0 \rightarrow 1)$ transition at the maximum does not occur in the directions of these principal axes. The angular

dependence of the resonance magnetic field, however, becomes so small that the lines of the various hyperfine splitting constants overlap with each other in the corresponding narrow range of the magnetic field. Consequently, the hyperfine splittings are completely smoothed out and the calculated A values are of no practical use.

Finally, we calculated the total line shapes according to the method by Taylor and Bray.¹⁶⁾ For the sake of simplicity we neglected the angular dependence of the transition probabilities. The patterns which were made up by neglecting the linewidths of all the transitions were convoluted with the Gaussian line shapes, and then numerically differentiated. As the absorption lines of the monomers overlap greatly with those of the dimers, it is impossible to fit the total line shapes of the calculated spectra to those of the observed ones. Therefore, we adjusted the magnetic parameters so that the parameters defined in Figs. 2 and 4 became consistent with those experimentally determined. Figures 7–11 suggest the ranges of the more exact parameters of the triplet dimers. Since the behavior of the hyperfine structures can be adequately explained by the parameters used for the calculations in Fig. 6, the true values will not deviate too much from them. We made them change gradually by the trial-and-error method, and finally obtained the spectra

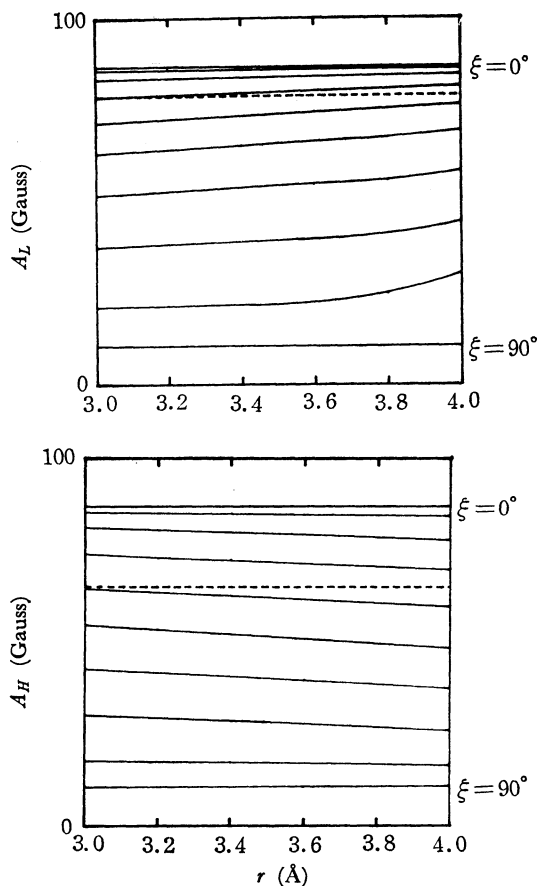


Fig. 8. The r and ξ dependence of A_L and A_H at X-band. $A_{//}=0.0090$ cm⁻¹, $A_{\perp}=0.0010$ cm⁻¹, $g_{//}=3.22$, $g_{\perp}=2.04$; Broken lines in the figure indicate the observed values of A_L and A_H ; A_L and A_H were calculated changing ξ at intervals of 10° .

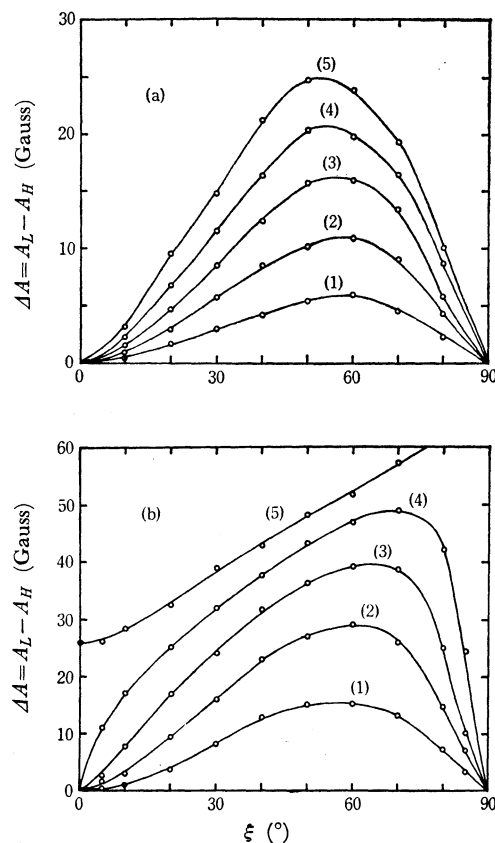


Fig. 9. The relation between $\Delta A = A_L - A_H$ and $\Delta g = g_L - g_H$ at different values of ξ . (a) X-band, (b) K-band; $A_{//}=0.0090$ cm⁻¹, $A_{\perp}=0.0010$ cm⁻¹, $g_{\perp}=2.05$, $g_{//}=(1), 2.10, (2), 2.15, (3), 2.20, (4), 2.25, (5), 2.30$.

shown in Fig. 10. The parameters determined from Fig. 10 are tabulated in Case B of Table 1; the magnetic parameters for the triplet dimer are shown below, with a rough estimation of the maximum errors:

$$g_{//} = 2.23 \begin{cases} +0.08 \\ -0.03 \end{cases} \quad g_{\perp} = 2.05 \pm 0.02$$

$$A_{//} = 90 \pm 5 \quad A_{\perp} = 10 \pm 5 \quad (\times 10^{-4} \text{ cm}^{-1})$$

$$r = 3.75 \begin{cases} +0.05 \\ -0.35 \end{cases} \quad (\text{\AA}) \quad \xi = 35^\circ \pm 5^\circ \quad \eta = 0^\circ$$

The agreement of the calculated spectra with the observed spectra is good in the low-field range. In the high-field range, however, the calculated intensity of the perpendicular component becomes larger and the calculated linewidth becomes smaller than those of the observed spectra. As a result, it seems that the hyperfine structures in this region appear only indistinctly.

The calculated spectra clearly show unusual hyperfine structures in the field range between the low-field parallel and perpendicular lines. The structures became more distinct in the K-band spectra. The perpendicular transitions occur when the static magnetic field is oriented along the direction perpendicular to the copper-copper axis. If the symmetrical axes of the g and D tensors are not coincident with each other, the perpendicular transition will split as a result of the anisotropy of the g tensor. Hence, the $\Delta M=1$ transitions do not show the typical pattern due to the axially symmetric tensors, and the stationary resonant field conditions for the low-field perpendicular transitions

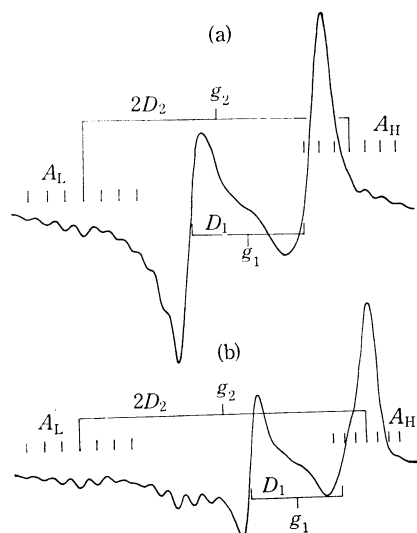


Fig. 10. The calculated ESR spectra of the triplet dimers of $\text{Cu}(\text{Mesal})_2$. (a) X-band, (b) K-band; $g_{//}=2.23$, $g_{\perp}=2.05$, $A_{//}=0.0090 \text{ cm}^{-1}$, $A_{\perp}=0.0010 \text{ cm}^{-1}$, $r=3.75 \text{ \AA}$, $\xi=35^\circ$; These spectra were convoluted by Gaussian line shapes, ($\Delta H=25 \text{ Gauss}$).

are satisfied at the angle of a considerably large hyperfine coupling constant.

Estimation of the Copper-Copper Distance. In the

above calculations, we neglected the effect due to the distributions of electron spins in their orbitals and the effect of pseudo-dipolar interaction. Taking this distribution effect into account will bring about a decrease in the estimated value of r , as was indicated by Chasteen and Belford.⁴⁾ Moreover, if a superexchange interaction through the oxygen atoms operates anti-ferromagnetically, the sign of the pseudo-dipolar interaction will become positive¹⁷⁾ and opposite to that of the real spin dipolar interaction. This effect may reduce the estimated value of r . However, the principal axes of the pseudo-dipolar interaction are directed along the direction parallel or perpendicular to the two coordination planes, rather than to the copper-copper axis.¹⁷⁾ If the total fine-structure tensor, \mathbf{D} , results mainly from the pseudo-dipolar interaction, the principal axes of the \mathbf{D} will be close to those of the g tensor. The calculated value of $\xi=35^\circ \pm 5^\circ$ suggests that the D value originates mostly from the real dipolar interactions. At any rate, the estimated value of r (3.75 \AA) will be the upper limit of the distance and the real value may possibly be smaller than this estimated value.

The authors would like to express their grateful acknowledgement to Dr. H. Yokoi for many helpful discussions and suggestions throughout this work.

17) B. Bleaney and K. D. Bowers, *Proc. Roy. Soc., Ser. A*, **214**, 451 (1952).